# Self-organizing Control of Urban Traffic Signal Based on Multiway Intersection Offset-setting Model

WISNU JATMIKO[1], ADI WIBOWO[2], ABDURRAHMAN S. K.[1],HERRY[1], A. A. KRISNADHI[1], ADE AZURAT[1]
T. FUKUDA[3], K. SEKIYAMA[3]
[1]Faculty of Computer Science, [2]Dept. of Informatics,[3]Dept. of Micro-Nano Systems Engineering
[1]Universitas Indonesia, [2]Diponegoro University,[3]Nagoya University
[1]Depok, Jawa Barat, [2]Semarang, Jawa Tengah,[3]Chikusa-ku, Nagoya
[1,2]INDONESIA, [2]JAPAN
wisnuj@cs.ui.ac.id

*Abstract:* This paper proposes a model of distributed self-organizing traffic control with self-organizing map in real situation. This model can be used as a general setting for controlling almost any type of intersection. It uses nonlinear coupled oscillator with multiway intersection and automatically adjusts the cycle time, split, and offset parameter of the controller. Results show increased speed and reduced delay under all traffic conditions.

*Keywords:* Urban Traffic Control, Distributed Self-organizing Control, Multiway Intersection

## 1 Introduction

Traffic control system is an important component of an intelligent transportation system which is aimed to manage flow of vehicles optimally such that congestions and accidents are avoided as much as possible. One of its principal application is implemented as a traffic signaling mechanism that minimizes delay when vehicles travel through several consecutive intersections. Such a system now has an increasingly significant role in the light of urbanization, population growth and increased motorization.

In an urban area where traffic density can easily lead to congestions and jams, a traffic signal network of relatively closely spaced intersections need to operate in a coordinated fashion. The main objective of such coordination is to regulate green times, i.e., the duration of the green signals, so that vehicles can travel through some adjacent signalized intersections without significant stops and delays. This is often difficult to achieve within an uncoordinated traffic signal network since the high traffic density frequently yields vehicle queues in front of an intersection that block other vehicles coming in from neighboring intersections. On the other hand, a coordinated signal network will provide a primary benefit of reduced vehicle stops and delays. Such benefits will allow the traffic to proceed more efficiently, allowing for energy conservation. Secondarily, a coordinated traffic signal network is able to regulate vehicle speed because signals are set so that more stops are incurred for vehicles that travel faster than the intended speed. Furthermore, such a coordinated network leads to a more efficient use of intersections by grouping vehicles into platoons [1].

There have been several approaches to solve the coordinated traffic signal control problem. Wei et al. presented a macroscopic two-dimensional cellular automata model of an urban traffic signal control system in which each intersection is regarded as a cell and the flow pressure is treated as the state [2]. Wang et al. used the rules of adaptive control system based on genetic study classification algorithm to solve the traffic signal's separated, complex, nonlinear features and prevent failure of the control rules in urban regional coordination traffic signal control system [3]. Also, Srinivasan et al. proposed multiagent systems based on online learning of fuzzy neural networks and hybrid computational intelligence techniques [4].

In this paper, we develop a coordinated traffic signal control system that is based on a distributed self-organizing map. The proposed system employs an entraintment model from Kuramoto [5] to synchronize signals at intersections.

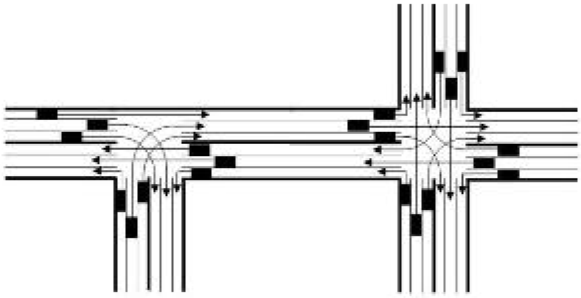

Figure 1: A real-world urban traffic net with multiway intersection

Our solution is a novel and nontrivial modification of the model in [6] by explicitly taking into account left and right turns and multiway intersections. The originating model itself has also been prototyped for real-world situations as described in [7, 8, 9]. However, it was not equipped to deal explicitly with left and right turns which are quite common in the real-world situations. The problem of dealing with left right turns has also been attacked by Sekiyama et al. They proposed a self-organizing route guidance system (SRGS) which cooperates with traffic signal control to handle left and right turns in an efficient manner [10]. However, such a guidance system relies on the information about the travel destinations of each vehicle; a requirement that is not always easy to satisfy in many situations. In addition, this approach assumed an idealized model of grid-like intersections and hence, not deal with multiway intersections which are common in the real world as shown in Fig. 1. We also provide simulation results in a complex map scenario which represents certain areas in Jakarta.

This paper is organized as follows. Section 2 describes basic approach of coordinated traffic signal control. Section 3 describes a development of signal network by nonlinear coupled oscillator with multiway intersection and adjustment of all the three parameters (cycle time, spilt and offset) based on the completely decentralized approach. Section 4 describes the simulation of the proposed model using a simulator software that we developed. The simulator also provides a visualization of the simulation to demonstrate the effectiveness of the proposed model under unstructured condition like in Indonesia. Results of simulation of the proposed model are given at the end of this section. The paper is concluded in Section 5 together with some remarks for future directions of this research.

## 2 Coordinated Traffic Signal Control

The common traffic signal parameters for controlling traffic flow are *cycle time*, *split* adjustment, and *offset*. We assume that a traffic signal completes one round of signaling that consists of a period of red signal and a period of green signal. Between the red and green signals, there may be a small, fixed period of clearance time, typically represented in real situations as a yellow signal. *Cycle time* denotes the time required for a signal between the start of a particular signaling round to the start of the signaling round that follows. *Split* is the fraction of the cycle time that is allocated to each phase for a set of traffic movements. *Offset* is the time difference between the beginning of green phases for a continuous traffic movement at successive intersections that may give rise to a *green wave* along an arterial [11].

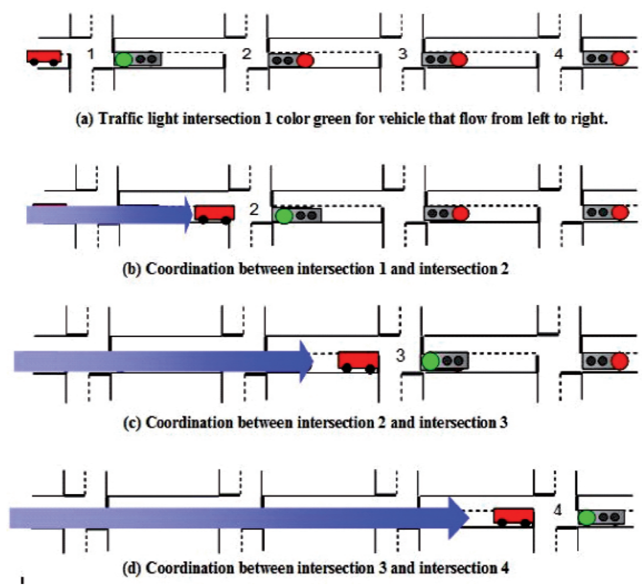


Figure 2: Coordination between nearest intersections for achieving the optimal flow of traffic.

In Fig. 2(a), a vehicle travels from intersection 1 to intersection 4. If the traffic light at intersection 1 is green, then intersection 1 will coordinate with intersection 2 to control the offset value. This will enable the vehicle to pass through without stopping at intersection 2, as seen in Fig.

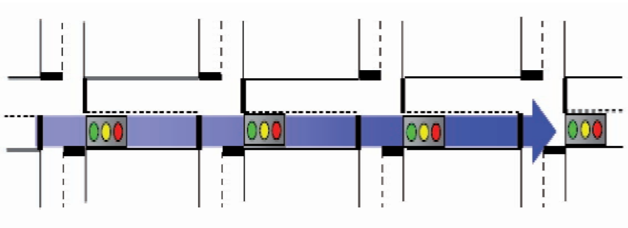

Figure 3: Traffic light control optimization result between nearest intersections

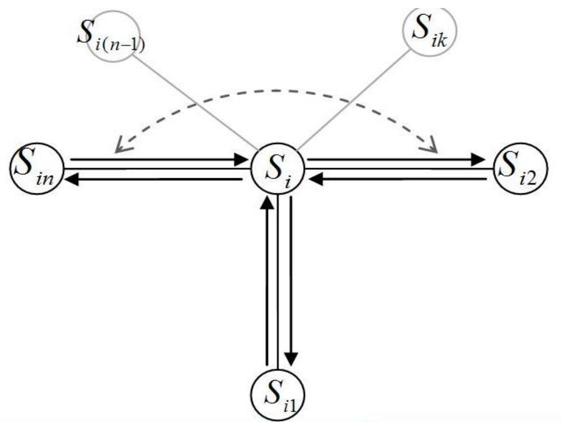


Figure 4: Bi-directed graph model for $n$-way intersection.

2(b). Likewise in Fig. 2(c) and Fig. 2(d), the vehicle can go without stopping at intersection 5 and 6, allowing it to attain an optimal velocity of the vehicles during its travel. The result of traffic light control optimization can be seen in Fig. 3.

# 3 Swarm Self-organizing Map

In the following, we describe the traffic signal network model based on swarm self-organizing map which generalizes for multiway intersections. Sekiyama et al. have presented the original, underlying model in [6] in which all intersections are always assumed 4-way with two main directions of traffic and arranged in a grid-like network. Here, we extend the model to $n$-way intersections and also taking into account left and right turns. For the sake of completeness, we will start first with the original derivation.

## 3.1 Traffic Signal Network Model

Consider a model of an urban traffic signal $S_i$ for a multiway intersection by bidirected graph as shown in Figure 4. The signal $S_i$ is $i$th signal in the coordinated signal network containing $N$ (possibly different types of) intersections. Each $S_i$ has a cycle time $T_i$ and $n_i$ neighboring signals $S_{ij}$, $j = 1, \ldots, n_i$. Note that each $S_{ij}$ which is defined as a neighbor of a particular $S_i$ is also a signal on its own with different value of $i$ in the network.

Let $\varepsilon_{ij}$ be the *normalized (incoming) traffic flow* from $S_{ij}$ to $S_i$, $i = 1, \ldots, N$, $j = 1, \ldots, n_i$, which is defined as follows:

$$\varepsilon_{ij} = \frac{1}{\rho_{im} \cdot T_i} \int_t^{t+T_i} \rho_{ij}(t) \cdot dt$$

$$\rho_{ij}(t) = \frac{1}{R_{ij}} \sum_{k=1}^{V_{ij}(t)} L_k^{ij}(t)$$

where:

- $\rho_{im}$ is the road capacity constant from $S_{ij}$ to $S_i$; note that the subscript $m$ is not an index value to signify a constant, unlike the $j$'s;
- $\rho_{ij}(t)$ is the (traffic) density from $S_{ij}$ to $S_i$ at a particular time $t$;
- $R_{ij}$ is the road length from $S_{ij}$ to $S_i$;
- $V_{ij}(t)$ is the number of vehicles in the road from $S_{ij}$ to $S_i$ at time $t$;
- $L_k^{ij}(t)$ is the length of the $k$th vehicle in the road between signal $S_{ij}$ and $S_i$ at time $t$; this value varies in time since the queue of vehicles in the road between $S_{ij}$ and $S_i$ also changes over time; .

## 3.2 Modelling Signal Network Using Nonlinear Coupled Oscillators

Let $\phi_i$ be the phase description of the signal $S_i$ given in its modulo-$2\pi$ value. Each signal $S_i$ is viewed as an oscillator whose dynamics is based on Kuramoto's model of nonlinear coupled oscillators and has the following generalized formulation based on phase description:

$$\dot{\phi}_i(t) = \frac{d\phi_i}{dt} = \omega_i + \frac{K}{n_i} \sum_{j=1}^{n_i} \varepsilon_{ij} \Gamma_i(\phi_i, \phi_{ij}) \qquad (1)$$

where $\Gamma_i$ is a periodic function such that

$$\Gamma_i(\phi_i, \phi_{ij}) = \Gamma_i(\phi_i + 2\pi, \phi_{ij}) = \Gamma_i(\phi_i, \phi_{ij} + 2\pi)$$

and $\omega_i = \dfrac{2\pi}{T_i}$ is the natural frequency of $S_i$.

From now on, we use a simple sinusoidal function in place of $\Gamma_i$ for the model in (1) as follows,

$$\dot{\phi}_i = \omega_i + \frac{K}{n_i}\sum_{j=1}^{n_i}\varepsilon_{ij}\sin(\phi_{ij}-\phi_i) \tag{2}$$

Euler's formula ($e^{i\theta} = \cos\theta + i\sin\theta$) implies that

$$\sin(\phi_{ij}-\phi_i) = \frac{e^{i(\phi_{ij}-\phi_i)} - e^{-i(\phi_{ij}-\phi_i)}}{2i}$$

which can be used to rearrange (2) as follows:

$$\begin{aligned}\dot{\phi}_i(t) &= \omega_i + \frac{K}{n_i}\sum_{j=1}^{n_i}\varepsilon_{ij}\frac{e^{i(\phi_{ij}-\phi_i)} - e^{-i(\phi_{ij}-\phi_i)}}{2i}\\ &= \omega_i + \frac{K}{2i}\Bigg(e^{-i\phi_i}\sum_{j=1}^{n_i}\frac{\varepsilon_{ij}}{n_i}e^{i\phi_{ij}}\\ &\qquad - e^{i\phi_i}\sum_{j=1}^{n_i}\frac{\varepsilon_{ij}}{n_i}e^{-i\phi_{ij}}\Bigg)\end{aligned} \tag{3}$$

If $A_i$ and $B_i$ are defined as follows,

$$A_i = \sum_{j=1}^{n_i}\frac{\varepsilon_{ij}}{n_i}e^{i\phi_{ij}} \qquad B_i = \sum_{j=1}^{n_i}\frac{\varepsilon_{ij}}{n_i}e^{-i\phi_{ij}} \tag{4}$$

Then (3) can be written as follows,

$$\dot{\phi}_i(t) = \omega_i + \frac{K}{2i}\left(e^{-i\phi_i}A_i - e^{i\phi_i}B_i\right) \tag{5}$$

Again, the Euler's formula can be used to rearrange (5) as follows:

$$\begin{aligned}\dot{\phi}_i(t) &= \omega_i + \frac{K}{2i}\Bigg((\cos\phi_i - i\sin\phi_i)A_i\\ &\qquad - (\cos\phi_i + i\sin\phi_i)B_i\Bigg)\\ &= \omega_i + \frac{K}{2i}\Bigg((A_i - B_i)\cos\phi_i\\ &\qquad - (A_i + B_i)i\sin\phi_i\Bigg)\end{aligned} \tag{6}$$

Then from (4), we obtain

$$\begin{aligned}A_i - B_i &= \sum_{j=1}^{n_i}\frac{\varepsilon_{ij}}{n_i}e^{i\phi_{ij}} - \sum_{j=1}^{n_i}\frac{\varepsilon_{ij}}{n_i}e^{-i\phi_{ij}}\\ &= \sum_{j=1}^{n_i}\frac{\varepsilon_{ij}}{n_i}2i\left(\frac{e^{i\phi_{ij}} - e^{-i\phi_{ij}}}{2i}\right)\\ &= 2\sum_{j=1}^{n_i}\frac{\varepsilon_{ij}}{n_i}i\sin\phi_{ij}\end{aligned} \tag{7}$$

$$\begin{aligned}A_i + B_i &= \sum_{j=1}^{n_i}\frac{\varepsilon_{ij}}{n_i}e^{i\phi_{ij}} + \sum_{j=1}^{n_i}\frac{\varepsilon_{ij}}{n_i}e^{-i\phi_{ij}}\\ &= \sum_{j=1}^{n_i}\frac{\varepsilon_{ij}}{n_i}2\left(\frac{e^{i\phi_{ij}} + e^{-i\phi_{ij}}}{2}\right)\\ &= 2\sum_{j=1}^{n_i}\frac{\varepsilon_{ij}}{n_i}\cos\phi_{ij}\end{aligned} \tag{8}$$

If,

$$a_i = \sum_{j=1}^{n_i}\frac{\varepsilon_{ij}}{n_i}\cos\phi_{ij} \qquad b_i = \sum_{j=1}^{n_i}\frac{\varepsilon_{ij}}{n_i}\sin\phi_{ij}$$

then (7) and (8) can be written as,

$$A_i - B_i = 2ib_i \qquad A_i + B_i = 2a_i$$

Thus, (6) is equivalent to

$$\dot{\phi}_i(t) = \omega_i + K\left(b_i\cos\phi_i - a_i\sin\phi_i\right) \tag{9}$$

With the Kuramoto's model, we aim for an entrainment condition of (2) which is modeled as

$$\dot{\phi}_i(t) = \omega_i + K\sigma_i\sin(\bar{\phi}_i - \phi_i) \tag{10}$$

where $\bar{\phi}_i$ is the weighted phase average of the neighboring signals.

Equating (9) and (10) using substraction formula of sines yields

$$\begin{aligned}b_i\cos\phi_i - a_i\sin\phi_i &= \sigma_i\sin(\bar{\phi}_i - \phi_i)\\ &= \sigma_i(\sin\bar{\phi}_i\cos\phi_i - \sin\phi_i\cos\bar{\phi}_i)\\ &= \sigma_i\sin\bar{\phi}_i\cos\phi_i - \sigma_i\sin\phi_i\cos\bar{\phi}_i\end{aligned}$$

We thus have for the coefficients of $\cos\phi_i$ and $\sin\phi_i$:

$$b_i = \sigma_i\sin\bar{\phi}_i \qquad a_i = \sigma_i\cos\bar{\phi}_i \tag{11}$$

It follows from (11) that

$$\sin\bar{\phi}_i = \frac{b_i}{\sigma_i} \quad \cos\bar{\phi}_i = \frac{a_i}{\sigma_i} \quad \tan\bar{\phi}_i = \frac{b_i}{a_i}$$

$$\bar{\phi}_i = \arctan\left(\frac{b_i}{a_i}\right) \qquad \sigma_i = \sqrt{a_i^2 + b_i^2} \tag{12}$$

### 3.3 Self-organization of Offset Settings

Our aim now is to apply the solution of the entrainment condition described in the previous subsection to derive the offset settings. The solution we will describe here is applicable for general $n$-way intersections, $n > 2$. For such $n$-way intersections, we first assume that each of $n$ incoming directions is provided with its own split time, i.e., each is considered to have an exclusive main phase. Within one main phase those, the corresponding incoming traffic flow may cross the intersection in all directions (go straight, turn right, turn left, etc.). Later on, we will provide the proposed solution with a feature that allows some of the phases combined for efficiency without necessarily ignoring some of the other phases. For example, this will allow the intersection to have green signal for two opposite directions so that both traffic flows may go in the straight direction at the same time. In particular, we will argue that this generalizes the model from [6] which only deals with 4-way intersections that have two main phases without explicitly taking into account vehicles that turn right or left.

Let $\psi_i$ be the relative phase between $\bar{\phi}_i$ and $\phi_i$, where

$$\psi_i = \bar{\phi}_i - \phi_i$$

Then the dynamics of the relative phase is expressed by

$$\dot{\psi}_i = \Omega_i - \omega_i - K\sigma_i \sin\psi_i \qquad (13)$$

where $\Omega_i$ is the natural frequency of $\psi_i$

The entrainment is reached whenever the phase value $\phi_i$ no longer changes with respect to the weighted phase average of all neighboring signals. Thus, this phase-locking condition of (13) occurs whenever $\dot{\psi}_i = 0$ which implies that

$$\sin\psi_i = \frac{\Omega_i - \omega_i}{K\sigma_i}$$
$$\psi_i = \arcsin\left(\frac{\Omega_i - \omega_i}{K\sigma_i}\right)$$
$$\left|\frac{\Omega_i - \omega_i}{K\sigma_i}\right| \leq 1$$

where $\sigma_i$ will be a constant $\tilde{\sigma}_i$ when oscillator $S_i$ is phase-locked with the neighboring signals. The

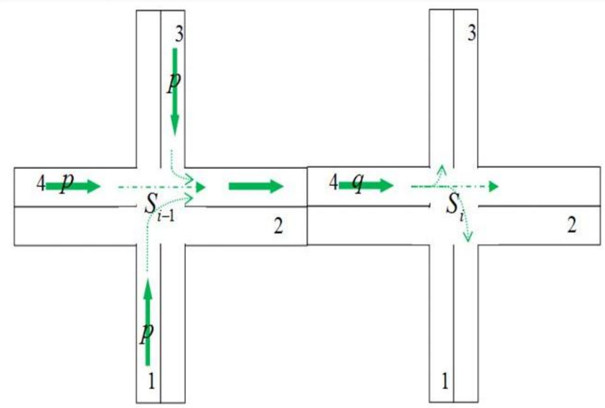


Figure 5: Possible values of $p$ in $S_{i-1}$ on a four-way intersection.

value of $\tilde{\sigma}_i$, according to (12), is given by

$$\tilde{\sigma}_i = \sqrt{\tilde{a}_i^2 + \tilde{b}_i^2}$$
$$\tilde{a}_i = \left(\sum_{j=1}^{n_i} \frac{\varepsilon_{ij}}{n_i} \cos\Delta\phi_{ij}\right)^2$$
$$\tilde{b}_i = \left(\sum_{j=1}^{n_i} \frac{\varepsilon_{ij}}{n_i} \sin\Delta\phi_{ij}\right)^2$$

where $\Delta\phi_{ij}$ is the phase difference between $\phi_{ij}$ and $\phi_i$ which is defined by

$$\Delta\phi_{ij} = \phi_{ij} - \phi_i \qquad (14)$$

To achieve the green-wave effect between two neighboring signals $S_i$ and $S_{i-1}$, the offset difference in (14) has to reach a value, say $\Delta\phi^*_{ij}$. In an $n$-way intersection, sources of an incoming traffic to $S_i$ from $S_{i-1}$ is assumed to be originated from the neighboring signals of $Si - 1$, except $S_i$. Hence, let $\underset{p\to q}{\Delta\phi^*_{ij}}$ be the desired offset between $\phi_{ij}$ and $\phi_i$ where in $S_i$, it corresponds to the $q$th split time $T_{i,q}$ and in the signal $S_{i-1}$, it corresponds to the $p$th split time. We derive $\underset{p\to q}{\Delta\phi^*_{ij}}$ below.

In Fig. 5 which describes the situation in a 4-way intersection, the source of incoming traffic from the direction indicated by $q = 4$ actually originate from the incoming traffic to $S_{i-1}$ labeled by $p \in \{1, 3, 4\}$. The problem is which value of $p$ is to choose. It is impossible to pick all possible value of $p$ because this will make the synchronization of all three directions into a single direction

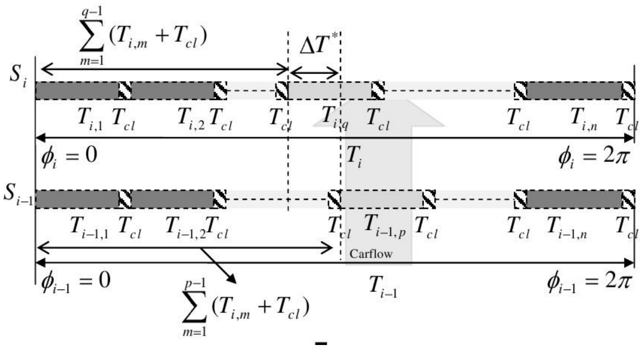


Figure 6: Offset-setting between successive signals for $p \to q$ direction before adjustment

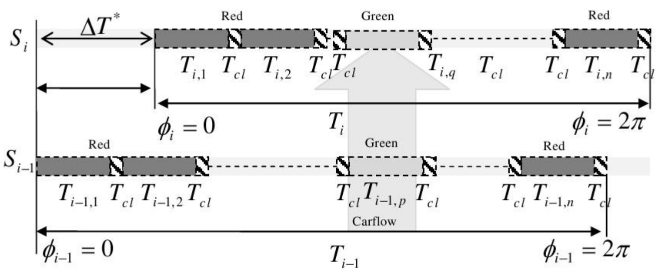


Figure 7: Offset-setting between successive signals for $p \to q$ direction, adjusted to green

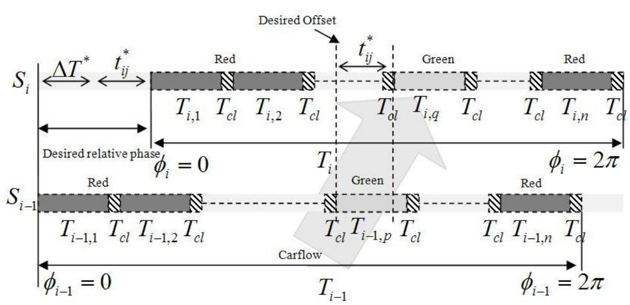


Figure 8: Offset-setting between successive signals for $p \to q$ direction, adjusted to green and travel time

$q$ impossible due to the fact that each of those directions begin at different phase. Hence, we are forced to choose one of the possible directions for $p$. In this model, the value $p$ is deliberately chosen to achieve appropriate offset settings of consecutive intersections along the path in the direction of heavy traffic to reduce delay at red lights.

Consider Fig. 6, 7, and 8. In order to derive the desired offset settings, we initially assume that both phases of $S_{i-1}$ and $S_i$ begin at the same time (Fig. 6) when entrained. We present the situation with respect to the whole cycle length of $2\pi$. Note that each signal has its own split settings, given by the values of $T$'s which will be derived later.

Suppose the green-wave is reached whenever the incoming traffic to $S_i$ in the $q$th direction is largely determined by the incoming traffic to $S_{i-1}$ in the $p$th direction. Thus, the green split that corresponds to $S_i$ in $q$th direction must start not earlier than the start of the green split that corresponds to $S_{i-1}$ in the $p$th direction. Let $T_{i-1,p}$ and $T_{i,q}$ be respectively the split time of $S_{i-1}$ in the $p$th direction and $S_i$ in the $q$th direction. Also, let $T_{cl}$ be the fixed duration of time clearances during transition from red to green and green to red. Then, as seen in Fig. 7, the start of $S_i$ must be shifted at least as much as $\Delta T^*$ which is defined as:

$$\Delta T^* = \Big(\sum_{m=1}^{p-1} T_{i-1,m} - \sum_{m=1}^{q-1} T_{i,m}\Big) + (p-q)T_{cl} \quad (15)$$

However, the formulation above does not yet take into account that vehicles may take a considerable amount of time to travel from $S_{i-1}$ to $S_i$. Hence, let $t^*_{ij}$ the expected time for a vehicle to reach $S_i$ from $S_{i-1}$ defined as

$$t^*_{ij} = \frac{l_{ij}}{v^{\max}_{ij}}$$

where $l_{ij}$ is the distance between adjacent signals and $v^{\max}_{ij}$ is the speed limit of the road between $S_{i-1} = S_{ij}$ and $S_i$. The desired offset between two successive signals is thus defined as

$$\underset{p\to q}{\Delta\phi^*_{ij}} = 2\pi \frac{t^*_{ij} + \Delta T^*}{T_i} \pmod{2\pi} \quad (16)$$

The desired offset above can then be used to obtain the desired relative phase, in accordance to (11), and (12), as follows

$$\Delta\bar{\phi}^*_i = \arctan\left(\frac{\sum_{j=1}^{n_i} \varepsilon_{ij} \sin \Delta\phi^*_{ij}}{\sum_{j=1}^{n_i} \varepsilon_{ij} \cos \Delta\phi^*_{ij}}\right)$$

Following (13), the desired natural frequency for signal $S_i$ can thus be expressed by the desired relative phase as

$$\omega^*_i = \Omega_i - \tilde{\sigma}^*_i K \sin \Delta\bar{\phi}^*_i$$

where $\Omega_i$ can be approximated as $\bar{\omega}_i$, the resulting compromised frequency of the signals when they are phase-locked [6].

### 3.4 Updating Natural Frequency

We assume initially the natural frequency of each signal $S_i$ is set with some initial value. For the desired natural frequency $\omega_i^*$, the natural frequency $\omega_i$ of signal $S_i$ is updated according to,

$$\omega_i(\tau_i+1) = \omega_i(\tau_i)+\alpha(\omega_i^* - \omega_i(\tau_i))+\beta(\tilde{\omega}_i^* - \omega_i(\tau_i))$$

where $\tau_i$ is the scaled time, $\alpha, \beta \in (0, 1)$ are positive constants and $\tilde{\omega}_i^*$ is some base frequency value for signal $S_i$ which is provided to prevent drift of natural frequency

### 3.5 Split Settings

Let $T_i(\tau_i)$ denote the cycle time of signal $S_i$:

$$T_i(\tau_i) = T_{i1}(\tau_i)+T_{i2}(\tau_i)+\cdots+T_{in}(\tau_i)+nT_{cl} \quad (17)$$

Here, $T_{cl}$ is the duration of clearance, and $T_{ik}(\tau_i), (k \in 1, 2, ..., n)$ are respectively split times from $S_i$ on $k$ direction. The split time $T_{ik}(\tau_i)$ is updated at the beginning of signal cycle in proportion to the sum of normalized amount of incoming traffic of every direction in $S_i$.

The normalized amount of incoming traffic for a direction is defined for $k = 1, \ldots, n_i$ by

$$r_{ik} = \varepsilon_{ik} \quad (18)$$

We can thus find the desired split time for direction $k$ for $k = 1, \ldots, n_i$ as

$$T_{ik}^* = \frac{r_{ik}(\tau_i)}{\sum_{m=1}^{n} r_{im}(\tau_i)}(T_i(\tau_i) - nT_{cl}) \quad (19)$$

and the updating function of split time $T_{ik}$ is defined for $k = 1, \ldots, n_i$ by

$$T_{ik}(\tau_i+1) = T_{ik}(\tau_i) + \gamma(T_{ik}^* - T_{ik}(\tau_i))$$

where $\gamma$ is updating constant, i.e., learning rate, that will determine how fast the current split time is moving to the desired split time.

### 3.6 Merging Directions into One Split Time

The intersection model discussed in previous section is intended for an $n$-way intersection where there are $n$ incoming traffic flow with its own different direction, and each is allowed for its own exclusive time to cross the intersection. This induces $n$ time splits for each direction in one cycle

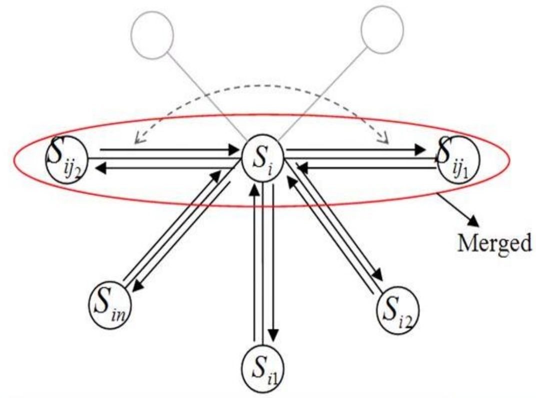


Figure 9: Direction of $S_{ij1}$ and $S_{ij2}$ is merged on same split.

of signaling. In real situation, we often find an $n$-way intersection where some directions are allowed to cross the intersection together. For example, a 4-way intersection may be arranged such that incoming traffic from two opposite directions are allowed to go straight during the same time split. This particular model was actually considered in the original paper from Sekiyama et al. [6] where a 4-way intersection is divided into two time split. Thus, our solution here generalizes the model there.

Consider an $n$-way intersection where $c$ directions are merged, $1 \leq c < n$ as illustrated in Fig. 9. Since there is a reduced number of split time, our split setting calculation has to be adjusted. adjustments to split setting calculation. The cycle time previously defined in (17) is modified into the following:

$$T_i(\tau_i) = T_i(\tau_i) + \cdots + T_{i\,(n-c)}(\tau_i) + (n-c)T_{cl}$$

The total incoming traffic flow of the merged directions is also taken into account. Thus, (18) must be modified appropriately. For example, in Fig. 9, it holds that $r_{ik} = \varepsilon_{ij_1} + \varepsilon_{ij_2}$ where the direction $k$ is formed as the combination of directions $j_1$ and $j_2$. In addition, the equation of split time for direction $k$ given in (19) has to be modified as follows:

$$T_{ik}^* = \frac{r_{ik}(\tau_i)}{\sum_{m=1}^{n-c} r_{im}(\tau_i)}(T_i - (n-c)T_{cl})$$

There is a problem however with merging some directions specified in this section. Consider again a 4-way intersection with incoming traffic from north, west, south, and east directions, and all vehicles travel on the left side of the road. Originally, there should be 4 splits in one cycle time. If we combine traffic that come from north and south direction into one split, then the traffic will be safe as long as all vehicles from north go to the south and all vehicles from south go to the north. This won't be the case if some vehicles from the north wish to turn right to the west direction or some vehicles from the south wish to turn right to the east direction. Those vehicles are not safe because there is no exclusive split which is allocated for them. In [10], this is solved by installing a route guidance system that interacts directly with the vehicles. We differ in this respect by avoiding such interactions with the vehicle. Our solution employs traffic signal phasing as described in the subsequent section.

### 3.7 Split Setting based on Traffic Signal Phasing

Recall that the intersection model described so far is based on a phase description in Kuramoto's model. Hence, one cycle can be considered as a sequence of signal phases. A traffic signal phase is a part of a cycle that is allocated to a stream of traffic or a combination of two or more traffic flows having the right-of-way simultaneously during one or more splits. The National Electrical Manufacturers Association (NEMA) has adopted and published precise nomenclature for defining the various signal phasing to eliminate misunderstanding between manufacturers and purchasers [12]. Fig. 10 illustrates the assignment of right-of-way to phases right-turn lanes by adapting NEMA phase numbering standards and the common graphic techniques for representing phase movements.

Our scheme based on traffic signal phasing is specified in the form of rules that determines phasing sequence, i.e., which directions should go at certain phases. Note that the NEMA phase numbering is only provided for 4-way intersections. We thus illustrate this scheme using its application on a 4-way intersection. Other types of $n$-way intersections can employ this scheme by first providing an appropriate numbering.

Consider a 4-way intersection (with incoming traffic from the north, south, west and east) whose signal is divided into two main phases which correspond respectively to horizontal and vertical directions of traffic flows. This means that in one cycle both north-to-south and south-to-north directions obtain the same green signal phase, and similarly, both east-to-west and west-to-east directions obtain the same green signal phase at the next split. Assume that vehicles travel on the left-side of the road, and every vehicle may turn left anytime at the intersection. Note that no green signal phase is dedicated solely for vehicles that turn right at the intersection. The formulation for split setting will be as follows.

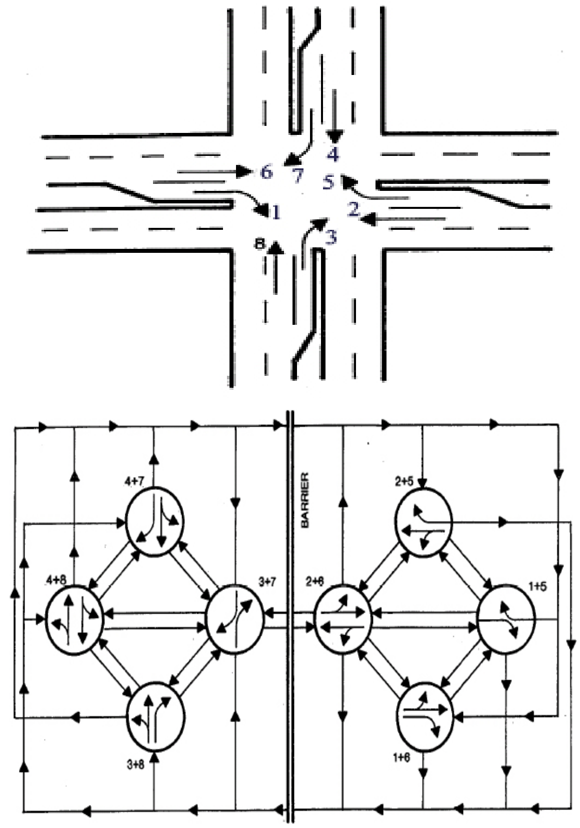


Figure 10: The traffic signal phasing for right-turn lane by adapting NEMA.

Let $T_i(\tau_i)$ denote the cycle time of signal $S_i$ which consists of two main phases. Then,

$$T_i(\tau_i) = T_{i1}(\tau_i) + T_{i2}(\tau_i) + 2T_{cl}$$

where $T_{i1}(\tau_i)$ is the split time of the main phase for the vertical direction, and $T_{i2}(\tau_i)$ is the split time of the main phase for the horizontal direction. $T_{i\ell}(\tau_i)$, $\ell = 1, 2$, is updated at the beginning of each signal cycle in proportion to the sum $r_{ik}$ of normalized amount of the incoming traffic for each directions.

$$r_{i1} = \varepsilon_{i1} + \varepsilon_{i3} \qquad r_{i2} = \varepsilon_{i2} + \varepsilon_{i4}$$

The desired split time for incoming traffic flows from horizontal and vertical direction is:

$$T^*_{i\ell} = \frac{r_{i\ell}(\tau_i)}{r_{i1}(\tau_i) + r_{i2}(\tau_i)}(T_i(\tau_i) - 2T_{cl})$$

The scheme presented above would be acceptable if there is only negligible amount of traffic that turns right at the intersection. In a real situation, this scheme forces any vehicles that wish to turn right to wait until it is safe to do so, i.e., when there is no vehicle going straight from the opposite incoming direction. In fact, this is the original scheme adopted in [6]. In Fig. 10, this two-phase signal combination corresponds to phases 2 and 6 and phases 4 and 8.

However, the above scheme is not sufficient when the amount of traffic turning right (phases 1, 3, 5, and 7) is not negligible. There will be an increased risk of collision and a longer vehicle delay which may cause traffic congestion. Our solution is thus to accomodate explicit allocation for those phases for turning right.

Let $\varepsilon_{i,k,a}$ be the traffic density of vehicles going straight (and turning left) and $\varepsilon_{ik,b}$ be the traffic density of vehicles turning right; both values are computed w.r.t., direction $k$, $k = 1, \ldots, 4$ (directions are labeled clockwise starting from the west). Then the split time of a main phase $T_{i\ell}$ in the previous scheme is divided into three smaller phases depending on which of the previous traffic densities dominates over the other. Define for $\ell = 1, 2$:

$$T^*_{i,\ell,a} = \frac{\varepsilon_{i,\ell,b}}{\varepsilon_{i,\ell+2,a} + \varepsilon_{i,\ell,b}}(T_{i\ell} - T_{cl})$$
$$T^*_{i,\ell,b} = \frac{\varepsilon_{i,\ell+2,b}}{\varepsilon_{i,\ell,a} + \varepsilon_{i,\ell+2,2}}(T_{i\ell} - T_{cl})$$

$T^*_{i,\ell,a}$ and $T^*_{i,\ell,b}$ are the measures reflecting how much traffic of vehicles turning right from both the opposite directions. $T^*_{i,\ell,a}$'s proportion w.r.t., $T^*_{i\ell}$ is determined by the ratio between traffic flow that turns right and the sum of traffic flow that turns right and traffic flow going straight from the opposite direction. Note that this sum is obtained from two traffic flows that cannot cross the intersection at the same time. Similarly, this also holds for $T^*_{i,\ell,b}$.

Now, the phase sequence is specified, depending on the time variable $\tau_i$, into the following cases as follows (see Fig. 10 for the phase numbering, and Fig. 11, 12 and 13 for description of each case). We assume w.l.o.g. that the time $\tau_i \in [0, T_{i\ell}]$. Also, $\ell = 1$ (resp. $\ell = 2$) indicates the horizontal (resp. vertical) direction. Note that in between changes of phase there is an

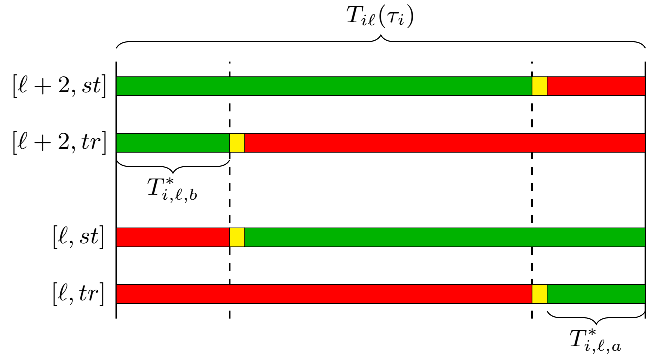


Figure 11: when $T^*_{i,\ell,a} + T^*_{i,\ell,b} < T_{i\ell}(\tau_i)$, sequence of phases is 2+5, 2+6, 1+6; or 4+7, 4+8, 3+8. Labels $st$ and $tr$ are resp. for going-straight signal and turn-right signal w.r.t direction $\ell$. See Fig. 10 for phase numbering.

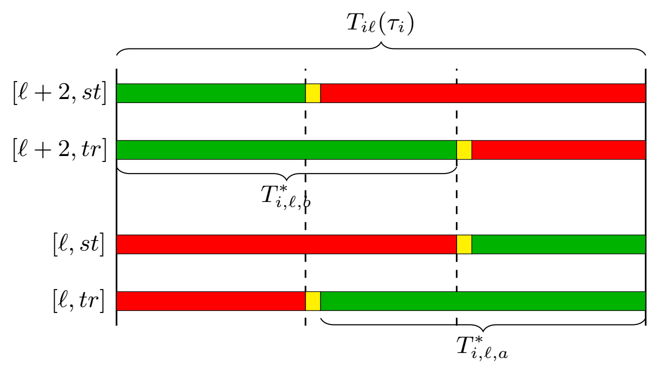


Figure 12: When $T^*_{i,\ell,a} + T^*_{i,\ell,b} > T_{i\ell}(\tau_i)$, the sequence of phases is 2+5, 1+5, 1+6; or 4+7, 3+7, 3+8.

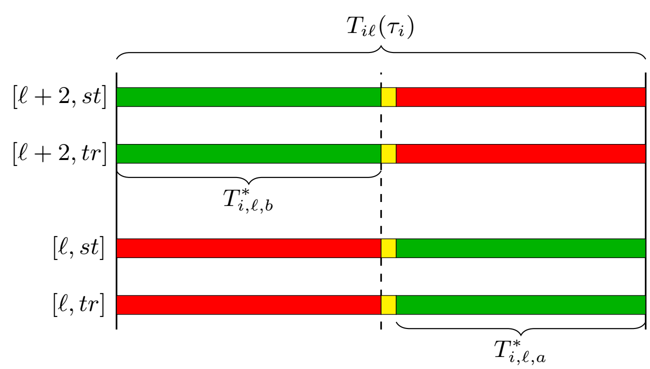


Figure 13: When $T^*_{i,\ell,a} + T^*_{i,\ell,b} = T_{i\ell}(\tau_i)$, the sequence of phases is 2+5, 1+6; or 4+7, 3+8.

interval for clearance.

1. Case $T^*_{i,\ell,a} + T^*_{i,\ell,b} < T_{i\ell}(\tau_i) - T_{cl}$:
   - $\tau_i \in [0, T_{i,\ell,a}]$: phase 2 and 5 if $\ell = 1$; phase 4 and 7 if $\ell = 2$
   - $\tau_i \in [T_{i,\ell,a} + T_{cl}, T_{i\ell} - T_{cl} - T_{i,\ell,b}]$: phase 2 and 6 if $\ell = 1$; phase 4 and 8 if $\ell = 2$
   - $\tau_i \in [T_{i\ell} - T_{i,\ell,b}, T_{i\ell}]$: phase 1 and 6 if $\ell = 1$; phase 3 and 8 if $\ell = 2$.
2. Case $T^*_{i,\ell,a} + T^*_{i,\ell,b} > T_{i\ell}(\tau_i) - T_{cl}$:
   - $\tau_i \in [0, T_{i\ell} - T_{cl} - T_{i,\ell,b}]$: phase 2 and 5 if $\ell = 1$; phase 4 and 7 if $\ell = 2$
   - $\tau_i \in [T_{i\ell} - T_{i,\ell,b}, T_{i,\ell,a}]$: phase 1 and 5 if $\ell = 1$; phase 3 and 7 if $\ell = 2$
   - $\tau_i \in [T_{i,\ell,a} + T_{cl}, T_{i\ell}]$: phase 1 and 6 if $\ell = 1$; phase 3 and 8 if $\ell = 2$.
3. Case $T^*_{i,\ell,a} + T^*_{i,\ell,b} = T_{i\ell}(\tau_i) - T_{cl}$:
   - $\tau_i \in [0, T_{i,\ell,a}]$: phase 2 and 5 if $\ell = 1$; phase 4 and 7 if $\ell = 2$
   - $\tau_i \in [T_{i,\ell,a} + T_{cl}, T_{i\ell}]$: phase 1 and 6 if $\ell = 1$; phase 3 and 8 if $\ell = 2$.

Obviously, the above rules only apply for 4-way intersections with two main phases. However, the idea can easily be extended to other types of $n$-way intersections with their own configuration of main phases.

# 4 Simulation

This section describes how a real-world traffic network was modeled using a microscopic simulation software and presents the results as compared against those obtained from fixed-time traffic signals. There are two main parts of the software, namely the traffic signal control system (TSCS) and the simulator. Fig. 14 depicts the relationship between TSCS and the simulator.

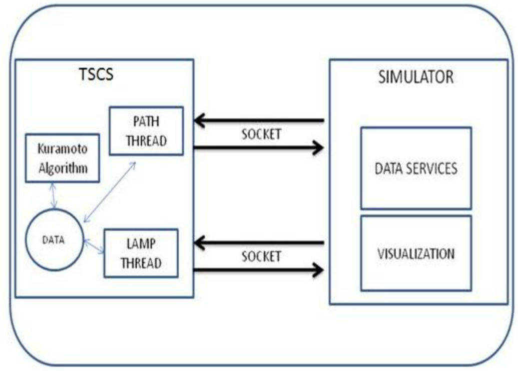


Figure 14: Relationship TSCS and Simulator.

## 4.1 The Traffic Signal Control System

The traffic signal control system (TSCS) is written in C with multithreading. The system calculate the traffic parameters of the entire traffic network once for every beginning of each signal cycle.

There are two kinds of threads for communication between TSCS and simulator: path threads and lamp threads. The path thread is responsible for obtaining traffic volume, average velocity of vehicles, and vehicle queue length at every intersection on simulator. On the other hand, the lamp thread is in charge of sending the traffic light signal data to the simulator. In this setting, whenever the TSCS needs some data with regards to certain intersections, it will send a data request through the path thread. The simulator then replies this request with the appropriate data. In the opposite direction, the lamp thread is employed by the TSCS to send the traffic light signal parameters to the simulator, so that it can update the cycle time of the traffic signals.

## 4.2 Traffic Simulator

The traffic simulator is part of the simulation software that also has a graphical user interface. The simulator is written in Java using Java component framework. It is developed in such a way that the designed or modeled traffic signal network can be implemented in the real world. The simulator maintains intersection threads for each intersection in the modeled signal network. The sampling rate for intersection threads is updated every 100 milliseconds. This enables intersection threads to make timely responses to the dynamically changing traffic network. During a simulation, the intersection threads are tuned to sample for traffic parameters from the traffic network once every one cycle time. Fig. 15 show the traffic simulator and TSCS running concurently. The inset shows the map of roads in certain Jakarta area with 9 intersections comprising 3-way, 4-way

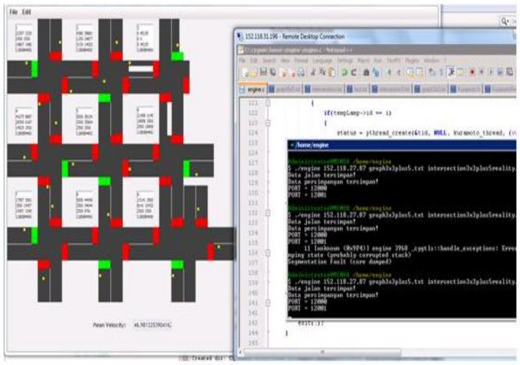

Figure 15: Running TSCS and Simulator.

Table 1: Details of the Simulation Parameter

| Symbol | Description | Value |
|---|---|---|
| $v_{ij}^{\max}$ | maximum speed | 60 Km/h |
| $K$ | coupling constant | 0.1 |
| $\alpha$, $\beta$ | rate of update of $w$ | 0.5, 0.05 |
| $\tilde{\omega}_i^*$ | base natural frequency | 0.1 |
| $\rho_{im}$ | road capacity | 36 cars/road |
| $\gamma$ | updating constant (learning rate) | 0.8 |

and 5-way intersections.

In the simulator, every intersection has information such as the path length between the street intersection, the vehicle velocity, cycle time signal phase, the number of vehicles passing through the intersection, road capacity and other intersection signal phase that are connected with this intersection. The value of simulation parameters is given in Table 1.

There are various scenarios to compare the effectiveness between the conventional method and the proposed method. There are two kinds of traffic network which represent real world condition of the traffic network system in Jakarta. The first kind of network, depicted in Fig. 16, represents of rather sparse networks of intersections found in certain regions in Jakarta. The second kind of network, as depicted in Fig 17, represents compact networks of intersections in Jakarta. In the traffic simulation, the following restrictions/conditions are applied.

1. Vehicle arrival follows a Poisson distribution.

Figure 16: Simple Map Scenario.

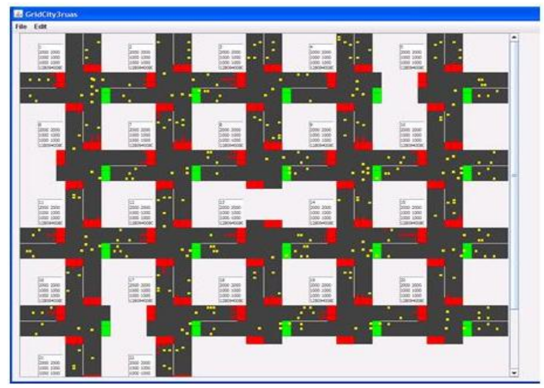

Figure 17: Complex Map Scenario.

2. The road capacity is 36 vehicle whose average length is 5 m (5 pixel in simulation).

3. The traffic capacity of Simple Map is 1400 vehicles per hour, and the complex Map is 5000 vehicles per hour.

4. Updates for traffic density is done every 20 seconds (short experiments) and 10 minute-scale (long experiments).

5. The minimum and maximum green times are 15 and 60 seconds, respectively.

### 4.3 Design of Experiments

Evaluations of the proposed model require a good and comparable benchmark against which the simulation results can be fairly compared. However, it turns out to be rather difficult, because unlike related works in [2, 3, 6, 8, 9], our solution strongly focuses on generalization to $n$-way intersections. This renders the results from those related works not directly comparable to our experimental results. In addition, the cycle time,

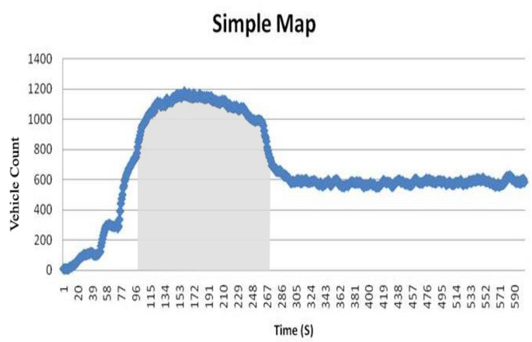


Figure 18: Density Distribution on 600 s in Simulator.

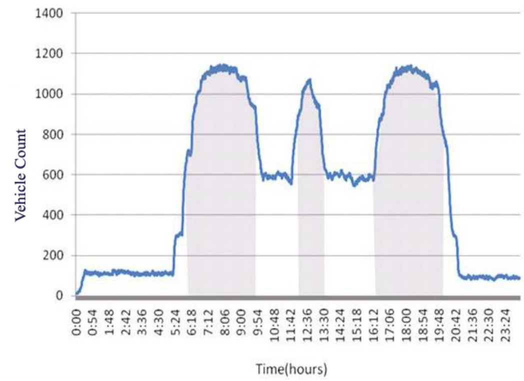


Figure 19: Density Distribution on 24 Hours Scenario in Simulator.

split time, and offset of traffic signals in Jakarta (the basis for our experiments) in the current traffic management system is set manually and kept fixed throughout their usage. Hence, it would be more realistic if the simulations are benchmarked against signal network with static settings.

Experiments are also designed to investigate influences of some novel features in the proposed model. First, for traffic of a particular incoming direction at an intersection, our model incorporate some parameters for offset setting that represents dominant source of that incoming traffic (the $p$ and $q$ parameters in Section 3.3). Secondly, the model is also extended with traffic signal phasing that allows split times merge. There will thus be experiments in which these affecting parameters are varied.

Overall, the experiments are done with respect to the two performance measures: (1) reduced vehicle delay on average; and (2) average velocity over all vehicles. Each experiment covers all of the three typical situations, namely in high, medium and low traffic density. High traffic density scenario is represents peak periods or rush hour. This period is a part of day in which traffic congestion and crowding on public transport are at their highest. Typically, this happens twice a day, once in the morning, and once in the evening, i.e., the times during which most people commute. Medium traffic density scenario represents normal condition. Normal condition happens in between peak times in the middle of the day. Low traffic density scenario represents traffic condition during the night.

There will be two kinds of simulations: short simulations of 600 seconds duration and long simulations of 24 hours duration, see Fig. 18 and 19. Both are given a similar number of vehicles. Short simulations are characterized with a single peak of traffic volume. Short simulations are also intended to verify that the computation of the simulator works well. Long simulations are characterized with multiple peak of traffic volume which represents multiple peak hours that may happen in the real situation.

Both simulations are tested for simple maps and complex maps with static settings or non-static settings. The scenarios for which non-static settings are applied, we vary the simulations on whether or not the offset is adjusted with dominant source of incoming traffic. For example, if the traffic from a neighboring signal is actually dominated by vehicles going straight (i.e., not turning right) at the neighboring signal, then using offset adjustment means that we set the variables $p$ and $q$ for Eq. (16) to represent this kind of traffic. Also, we vary on whether or not there are some incoming directions are merged (and thus applying traffic signal phasing). To mirror the real situation, the merge is done on two incoming traffic from opposite directions so that it is possible for vehicles going straight from both traffic are able to cross the intersection during the same green phase.

The simulation of the occurrence of accidents on the map, we made occurring the stalled vehicle in several roads. In this case make the long queue of vehicles occurred on the road. Moreover causing other vehicles from crossing the street can not get into this road. In this simulation is not traffic detour of the vehicle, but by default the vehicle will move into an empty lane from the jammed roads.

### 4.4 Simulation Results

Table 2 and 3 provide the results of simulation as an average over separate runs of experiment. We argue that this a reasonable presentation of typical results because the variances for all cases are sufficiently small. The tables list results from four kinds of scenario: 600s Straight-Dominant, 600s Right-Dominant, 24h-Straight-Dominant, and 24h-Right-Dominant. The Straight-Dominant types indicate that the traffic in simulation is arranged so that at each intersection, the number of vehicles going straight dominates the number of vehicles that turn right or left. Meanwhile, the Right-Dominant types indicate the opposite condition.

Both tables are arranged into columns that describe experiments with traffic signal in static settings, and traffic signaling with our self-organizing scheme, either without or with adjusting offset with respect to dominant source of incoming traffic. The simulations done using self-organizing scheme are further categorized into whether or not the signaling phases of some incoming traffic are merged using the scheme described in Section 3.6 and 3.7. Finally, in all cases, we do simulations in both simple and complex maps as described by Fig. 16 and 17 (indicated by S for simple maps and C for complex maps).

For the 600s-scenarios which simulates typical situation of morning rush hour with one peak, we do 30 separate runs with different Poisson seeds for each category. The results given by the first two rows of each table are positive. In particular, our model that also employs offset adjustment and merge of signal phases yields higher average of vehicles' velocity and lower delay for each map type. In our model, the results mean that on average, a vehicle travels up to ca. 4 minutes faster for a 10km trip. For vehicle's delay at intersections, the results also provide reduced delay i.e., the delay between 13% upto 56% shorter than that of the static settings. The results are also consistent in the sense that in both cases of Straight-Dominant and Right-Dominant, our model always scores better performance for each map type. In addition, using offset adjustment is always better than without using it, and merging some of signal phases typically improves the result.

Next, the 24h-scenarios are presented as the last two rows of each table. These scenarios simulate real traffic situation over 24 hours where there can be several peaks (heavy traffic) interleaved with normal or light traffic conditions. The scenarios are realized with 6 separate runs for each category. In comparison to the 600s-scenarios, the 24 hours duration provides a more difficult challenge because many more possibilities for complex traffic situations to occur. Despite that, the results are still positive and of similar tendency to those of the 600s-scenarios, albeit with a slightly smaller gain. In these scenarios, our model also scores better performance for each map type. We can also see that using offset adjustment and merging some signal phases improve the results. The gain for velocity is slightly smaller especially for the Right-Dominant type, whereas the reduction in delay is in between 13% and 42% shorter than that of static settings.

The comparison of the results of the traffic arrangements during an accident can be seen in table 4. The results show that the proposed method increases the vehicle velocity when the accident occurs. This happens due to long queues of vehicles at particular street led to the reduction of green time which direction into this street. Therefore, by default the vehicle will move to the lane which gives a longer green time at the adjacent intersections.

## 5 Conclusion

We have presented a model of self-organizing control for urban traffic signal which is suitable for general $n$-way intersections. The model has been succesfully prototyped and tested in both simple and complex traffic network. The simulation results has proved that the proposed model yields better performance than static and fixed signaling systems which are commonly implemented. In particular, the simulations demonstrated that the proposed model is able to improve the average velocity of vehicles, and at the same time, reduce vehicles' delay at intersections. The proposed model is also sufficiently robust and efficient in peak periods or rush hour. However, further study and experimental data is needed in order to provide a

Table 2: Average vehicles' velocity (in km/h)

| Scenarios | Static method | | Self-organizing traffic signal network | | | | | | | |
|---|---|---|---|---|---|---|---|---|---|---|
| | | | Offset unadjusted | | | | Offset adjusted | | | |
| | | | without merge dir. | | with merge dir. | | without merge dir. | | with merge dir. | |
| | S | C | S | C | S | C | S | C | S | C |
| 600s: Straight-Dominant | 18.43 | 18.462 | 18.676 | 18.809 | 18.865 | 19.408 | 20.31 | 20.536 | 20.735 | 21.064 |
| 600s: Right-Dominant | 18.775 | 18.778 | 19.218 | 19.741 | 19.041 | 19.39 | 20.59 | 20.788 | 20.405 | 20.415 |
| 24h: Straight-Dominant | 22.87 | 21.757 | 22.966 | 22.872 | 23.194 | 22.921 | 25.245 | 24.318 | 25.56 | 24.859 |
| 24h: Right-Dominant | 23.865 | 22.720 | 24.427 | 24.116 | 24.203 | 23.042 | 25.61 | 24.721 | 25.15 | 23.124 |

Table 3: Average vehicles' delay at intersections (in s)

| Scenarios | Static method | | Self-organizing traffic signal network | | | | | | | |
|---|---|---|---|---|---|---|---|---|---|---|
| | | | Offset unadjusted | | | | Offset adjusted | | | |
| | | | without merge dir. | | with merge dir. | | without merge dir. | | with merge dir. | |
| | S | C | S | C | S | C | S | C | S | C |
| 600s: Straight-Dominant | 90.18 | 167.06 | 85.931 | 149.934 | 76.074 | 131.523 | 72.31 | 85.96 | 70.21 | 73.5 |
| 600s: Right-Dominant | 97.15 | 197.26 | 92.569 | 192.049 | 88.208 | 172.368 | 75.13 | 110.12 | 81.43 | 142.4 |
| 24h: Straight-Dominant | 263.82 | 504.04 | 248.0194 | 457.898 | 232.295 | 429.389 | 236.49 | 316.79 | 229.92 | 296.43 |
| 24h: Right-Dominant | 312.69 | 598.41 | 297.952 | 559.843 | 286.705 | 541.939 | 248.07 | 397.05 | 262.89 | 510.51 |

real-scale implementation of the model on traffic signaling devices. It is also noted that any working implementation of the proposed model necessitates an accompanying traffic monitoring system that is able to provide traffic data required by the proposed model.

**Acknowledgements:** This work was supported in part by the Incentive Research by the Ministry of Research and Technology Republic of Indonesia 2010 and Riset Unggulan Universitas Indonesia 2011.

## References

[1] M. Kutz. *Handbook of Transportation Engineering*. McGraw-Hill handbooks. McGraw-Hill, 2004.

[2] Junhua Wei, Anlin Wang, and N. Du. "Study of Self-organizing Control of Traffic Signals in an Urban Network Based on Cellular Automata". In: *IEEE Transactions on Vehicular Technology* 54.2 (Mar. 2005), pp. 744–748.

[3] Anlin Wang, Xiaofeng Wu, Bo Ma, and Chenglin Zhou. "Rules Self-Adaptive Control System for Urban Traffic Signal Based on Genetic Study Classification Algorithm". In: *International Conference on Artificial Intelligence and Computational Intelligence, 2009 (AICI '09)*. Vol. 1. Nov. 2009, pp. 429–433.

[4] D. Srinivasan, Min Chee Choy, and R. L. Cheu. "Neural Networks for Real-Time Traffic Signal Control". In: *IEEE Transactions on Intelligent Transportation Systems* 7.3 (Sept. 2006), pp. 261–272.

[5] Y. Kuramoto. *Chemical Oscillations, Waves, and Turbulence*. Chemistry Series. Dover Publications, 2003.

[6] K. Sekiyama, J. Nakanishi, I. Takagawa, T. Higashi, and T. Fukuda. "Self-organizing Control of Urban Traffic Signal Network".

Table 4: Average vehicles' velocity when Accicent (in km/h)

| | Simple Map | | Complex Map | |
|---|---|---|---|---|
| Traffic Flow | Static Method | Self-organizing | Static Method | Self-organizing |
| Low | 21.13 | 22.77 | 23.05 | 22.92 |
| Medium | 20.57 | 22.09 | 19.67 | 22.15 |
| Heavy | 18.24 | 19.03 | 18.87 | 19.98 |

In: *IEEE International Conference on Systems, Man, and Cybernetics, 2001*. Vol. 4. 2001, pp. 2481–2486.

[7] W. Jatmiko, F. Heriyadi, A. A. Krisnadhi, I. Takagawa, K. Sekiyama, and T. Fukuda. "Distributed Traffic Control with Swarm-Self Organizing Map in Jakarta: Simulation and Measurement". In: *International Symposium on Micro-NanoMechatronics and Human Science, 2009. MHS 2009*. Nov. 2009, pp. 598–601.

[8] W. Jatmiko, F. Heriyadi, A. A. Krisnadhi, I. Takagawa, K. Sekiyama, and T. Fukuda. "Distributed traffic control with swarm-self organizing map in Jakarta: Progress and Challenge". In: *International Symposium on Robotics and Intelligent Sensors (IRIS 2010)*. Nagoya, Japan, Mar. 2010.

[9] W. Jatmiko, A. Azurat, Herry, A. Wibowo, H. Marihot, M. Wicaksana, I. Takagawa, K. Sekiyama, and T. Fukuda. "Self-Organizing Urban Traffic Control Architecture with Swarm-Self Organizing Map In Jakarta: Signal Control System and Simulator". In: *International Journal on Smart Sensing and Intelligent Systems* 3.3 (2010), pp. 443–465.

[10] Kosuke Sekiyama and Yasuhiro Ohashi. "Distributed Route Guidance Systems with Self-Organized Multi-Layered Vector Fields". In: *JACIII* 9.2 (2005), pp. 106–113.

[11] N. J. Garber and L. A. Hoel. *Traffic and Highway Engineering*. Cengage Learning, 2009.

[12] Robert L. Gordon and Warren Tighe. *Traffic Control Systems Handbook*. Tech. rep. FHWA-HOP-06-006. Washington, DC.: Office of Transportation Management, Federal Highway Administration, Oct. 2005.